Transactions of the SMiRT 27
Yokohama, Japan, March 3-8, 2024
Division III

ENERGY BASED QUASI-STATIC DROP LOAD STUDY OF A SPENT FUEL POOL STRUCTURE

Bojan Radmanović[1], Adam Fila[2], Burkhard Wienand[3]

[1] Expert Engineer, Framatome GmbH, Karlstein, Germany (bojan.radmanovic@framatome.com)
[2] Senior Expert Engineer, Framatome GmbH, Karlstein, Germany
[3] Senior Expert Engineer, Framatome GmbH, Karlstein, Germany

ABSTRACT

One of the events which might jeopardize the structural integrity and functionality of a spent fuel pool (SFP) is a drop of a heavy object on the bottom slab. This paper discusses the assessment of the damage state of the concrete structure caused by the drop load. Emphasis is made on the constitutive modelling of the concrete material and the energy based quasi-static drop load analysis methodology, as well as the sensitivity analysis of the effects of the strength ratio of the 2nd to 1st phase concrete layer on the structural response. Simulation strategy is based on the explicit finite element (FE) solver using quasi-static analysis and an augmented Riedel–Hiermaier–Thoma (RHT) concrete constitutive model providing the optimal trade-off between the accuracy, efficiency, robustness and convergence for the problems analysed. Sensitivity studies indicate that low strength ratio of the 2nd to 1st phase concrete acts favourably to the mechanical behaviour of the system. Low 2nd phase concrete strength allows the impact energy to be absorbed and dissipated by the local high inelastic deformations and damage of 2nd phase concrete layer. By balancing the strength ratio of 2nd to 1st phase concrete it is possible to protect the 1st phase concrete layer from extensive cracking and damage, with 2nd phase concrete layer acting as a cushion, containing the damage within.

DESCRIPTION OF THE PROBLEM

Introduction

A SFP typically comprises reinforced concrete walls and bottom slab covered with steel liner (Figure 1). Liner is made of thin steel sheets, anchored to the SFP structure by the steel framework assembly (profiles, anchorage, etc.). A SFP bottom slab is made of two layers, primary (1st phase) and secondary (2nd phase) concrete, with 1st to 2nd phase layer thickness ratio of about 10. Thick 1st phase concrete layer provides the main global structural integrity to the SFP and contains reinforcement to resist various mechanical and thermal actions. 2nd phase concrete layer lies on top of the 1st phase layer and serves mainly as the finishing layer as well as the to provide the local structural support for the liner and the anchoring framework.

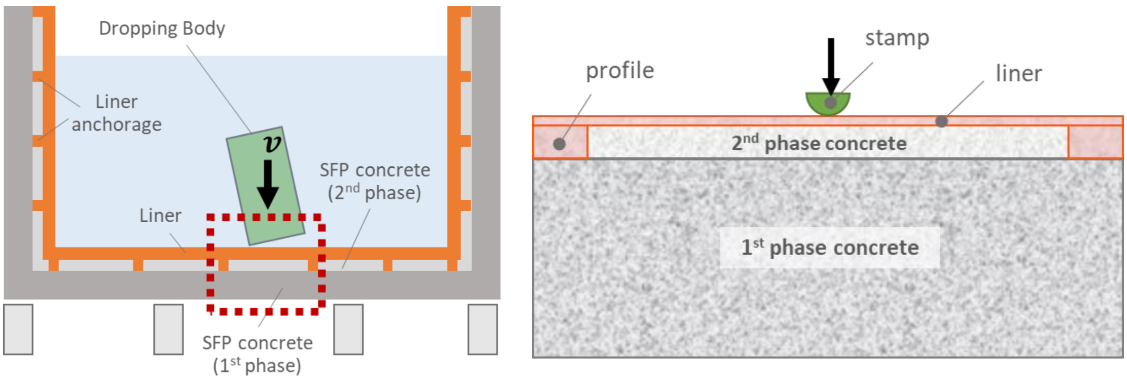

Figure 1. System sketch of a SFP subjected to a heavy body drop load: (a) Global; (b) Local view.

During the transport of a heavy load trough the storage area in the pool, heavy object which can weigh several tens of tons might detach from its supports and drop on the top of the SFP bottom slab, possibly jeopardizing the structural integrity and functionality of the spent fuel pool.

The main objective of the current study is an assessment of the damage state of the concrete SFP structure subjected to a load caused by the drop of the heavy object. This comprises assessment of the mechanical behaviour or the supporting SFP structure, identification of the critical areas and load scenarios, assessment of the damage of the 1st and 2nd phase concrete layer, sensitivity studies on the effect the 2nd to 1st phase concrete strength ratio on the mechanical behaviour of the pool structural system, as well as evaluation of the load-displacement and energy curves. Detailed assessment of the liner damage is outside of the scope of the present study.

Drop Load Scenarios

It is assumed that the heavy body with mass m is vertically dropping from height h above the liner. Conservatively the influence of the water is neglected resulting in the kinetic energy just before the impact

$$E_{impact} = E_{kinetic} = \frac{1}{2} m \cdot v_{impact}^2 = mgh = E_{im} \,. \tag{1}$$

Considering that the falling heavy body will always be completely submerged in water, this value of the impacting kinetic energy is very conservative since it neglects the Archimedes' and drag effects of the water on the impact velocity. For example, considering only the Archimedes' effect the impact velocity would be reduced by 35% resulting in the corresponding reduction of the impact energy by 87%.

Drop of the body in the middle of the liner sheet, i.e. in-between the framework, is analysed (see Figure 1b). Different drop load scenarios, depending on inclination and the position of the impact area, are analysed. In the current paper only the case with the body corner drop is presented (see Figure 2).

Impacting body (stamp) is assumed to be rigid (hard impact). The load is applied in form of the prescribed vertical displacements in a quasi-static analysis and the impacting area does not change significantly, since the kinematics of the dropping body (rotation, sliding and rolling) are not considered.

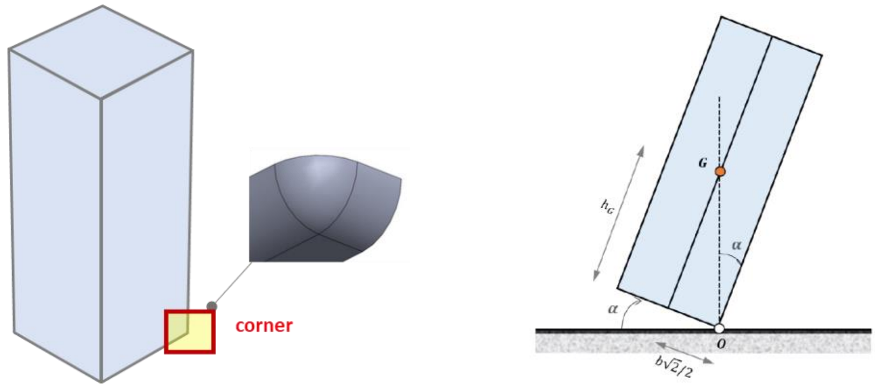

Figure 2. Drop load: (a) Drop position and impact area; (b) Dropping body inclination.

Consideration of the Drop Load Analysis Using Simplified Methods

Different engineering guidelines such as CEB (1988) or RCC-CW (2020) provide directions on how to analyse the concrete structures subjected to drop loads. These guidelines are mostly based on the engineering methods and simplified rheological models.

Both aforementioned codes start from the same premise based on the punching shear body resistance, as outlined in Figures 3 and 4. As show in the Figure 3a, the model consists of a simple two- or three-mass rheological models. For example, in the two-mass-model, two non-linear springs $R_1(u)$ and $R_2(u)$ represent, respectively, the deformation characteristics of the surrounding plate in bending and the punching cone relative to the surrounding plate. Under monotonically increasing vertical deformation $u(t)$ the total punching cone resistance $R_2(u)$ can be described by the backbone curve shown in Figure 3b and typically consists of three contributing factors [RCC-CW (2020)]: concrete tensile strength along the cone boundaries $R_{cys,b}$, stirrups $R_{cs,a}$ and bending reinforcement $R_{cl,b}$.

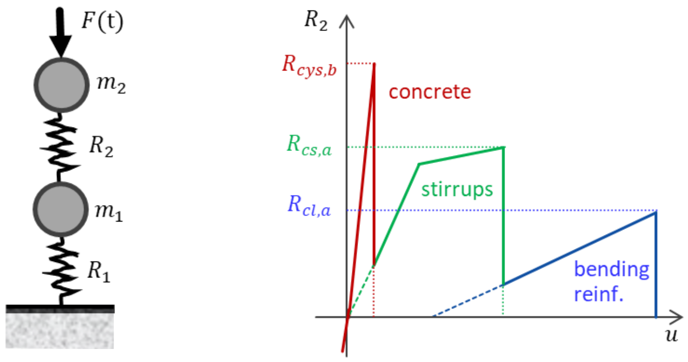

Figure 3. (a) Two-mass rheological model for drop load analysis; (b) Resistance-displacement diagram according to RCC-CW.

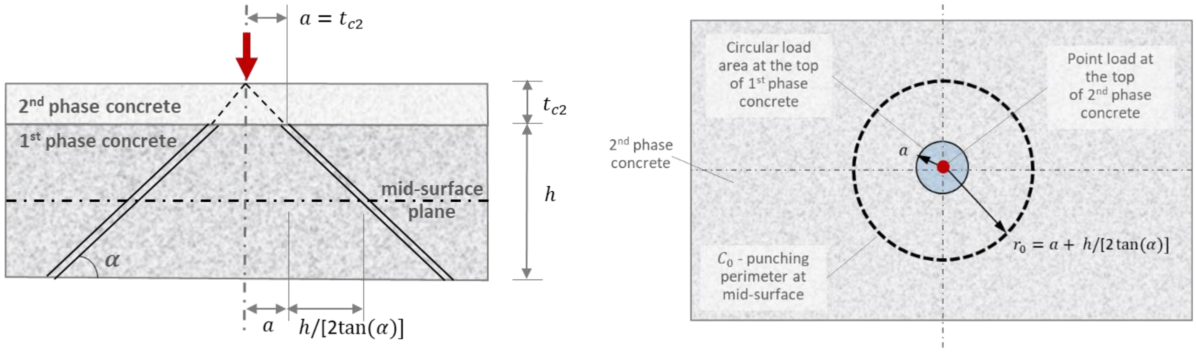

Figure 4. Geometry of the punching cone body: (a) Side view; (b) Top view.

These engineering models have been known to provide realistic results for the global consideration and ultimate limit state calculations of the drop loads analysis, see Fila et al. (2015) for instance. In the present study however magnitude of the applied impacting forces is below the level of the concrete contribution to the slab punching shear resistance $R_{cys,b}$. Thus, the punching shear body never fully forms and the global displacements of the 1st phase concrete remain very low. The deformation and energy dissipation are mostly localized in the proximity of the impact zone and governed by the cracking and crushing of the 2nd phase concrete. For these reasons, simplified methods which are based on the global consideration of the punching cone resistance are not well suited for the current study. Thus, more detailed simulation analysis capable of considering high local damage effects of the concrete is employed.

Contribution of the shear and bending reinforcement to the punching resistance takes affect only after large displacements have taken place, i.e. after the full forming of the punching cone. However, in this study, due to the fact that the deformations of the 1st phase concrete remain very low, reinforcement will not be considered.

Although in the current study the validity of the simplified global method is not justified, the analytical formulas in RCC-CW and CEB are used to assess the order of magnitude of the contribution of the concrete to the resistance of the punching cone $R_{cys,b}$.

Taking into account the concrete tensile strength along the cone boundaries, the slab punching concrete resistance $R_{cys,b}$ according to RCC-CW (2020) can be computed as:

$$R_{cys,b} = C_0 \cdot \bar{V}_{fd} \,, \tag{2}$$

where C_0 represents the perimeter of the punching slab body at the mid-surface (centroidal) plane of the slab. $\bar{V}_{fd}$ is the concrete contribution to shear resistance per unit length of the punching perimeter

C_0, given in Appendix DH 6000 of RCC-CW. The punching body geometry in most general case is defined by the following parameters, see Figure 4a:

- Geometry of the impact area. In case of the circular impact area, geometry is defined by the radius denoted as a;
- Thickness of the slab h;
- Angle of the punching body α. In most general case $\alpha \leq 40°$.

Conservatively assuming that the drop load acts as a point load on the top of the 2nd phase concrete of thickness t_{c2}, the diameter of the of the impacting area on the top of the 1st phase concrete can be approximated by $2a = 2t_{c2}$. The expected punching body geometry for corner impact is assumed to be according to Figure 4.

Comparing the slab punching concrete resistance computed according to CEB provisions with the resistance computed according to RCC-CW there is a difference by the factor of about 2 in favour of CEB provisions. In reality this resistance is difficult to estimate due to large scatter of the concrete's tensile strength.

Chosen Analysis Method and Summary of Main Assumptions

Different simulation strategies have been considered and an energy based quasi-static method is chosen as an optimal solution based on the project requirements and constraints.

Thus, in this particular study, time-dependent effects are neglected and the drop load is considered as the equivalent quasi-static load applied as an imposed displacement on the rigid impactor body (hard impact). Reinforcement of the 1st and 2nd phase concrete is neglected. The initial inner stress and strain state as well as damage of the pool concrete structure and liner prior to the drop load event are not explicitly considered in the drop load simulation analysis in the current study.

Energy based method is employed, i.e. the structure is able to sustain the impact if the dissipation energy (equal to plastic work) of the structure is higher than the kinetic energy of the impact, i.e.:

$$E_{disipation} = W_{pl} \geq E_{im} . \tag{3}$$

In addition, main concrete structural system should maintain the structural integrity after the drop load event, i.e. 1st phase concrete should not experience local punching shear failure. Limited and controlled local damage in the concrete is necessary in order for the structure to be able to dissipate impacting energy. Damage of the concrete is assessed at three analysis states with W_{pl}/E_{im} ratio equal to 1.0, 1.25 and 1.5.

Simulation strategy is based on the explicit FE solver using quasi-static analysis and an augmented RHT concrete material model providing the optimal trade-off between the accuracy, efficiency, robustness and convergence for the problems analysed. The chosen methodology is well suited for the what-if studies and qualitative assessment of mechanical behaviour and concrete damage in the conceptual design phase.

Considering all the conservative assumptions which are not related to the nature (quasi-static or dynamic) of the analysis (in particular neglecting the effects of fluid on the velocity of the falling body, realistic kinematics of the dropping body after the impact, flexibility and energy dissipation potential of the impacting dropping body, etc.) it is reasonable to presume that most of the results in the current study, especially those related to the overall structural integrity, are generally conservative.

SIMULATION MODEL

Geometry, Boundary Conditions, Connections and Finite Element Mesh

As already described, local effects in the proximity of the impact zone are governing the mechanical behaviour of the system. This implies that the local model with appropriate boundary conditions is sufficient to represent the mechanical behaviour of the system. Framework profiles are at a significant distance away from the impact zone and are not considered in the present study.

Figure 5a shows a simulation geometry for corner impact case, resulting from domain sensitivity tests performed in order to localize the problem and to determine an appropriate domain size.

Appropriate symmetry boundary conditions (BC) are applied on the symmetry planes (1/2 symmetry for corner impact). Bottom face of the 2nd phase concrete is free and side faces boundary conditions are defined as fixed displacements (see Figure 5b).

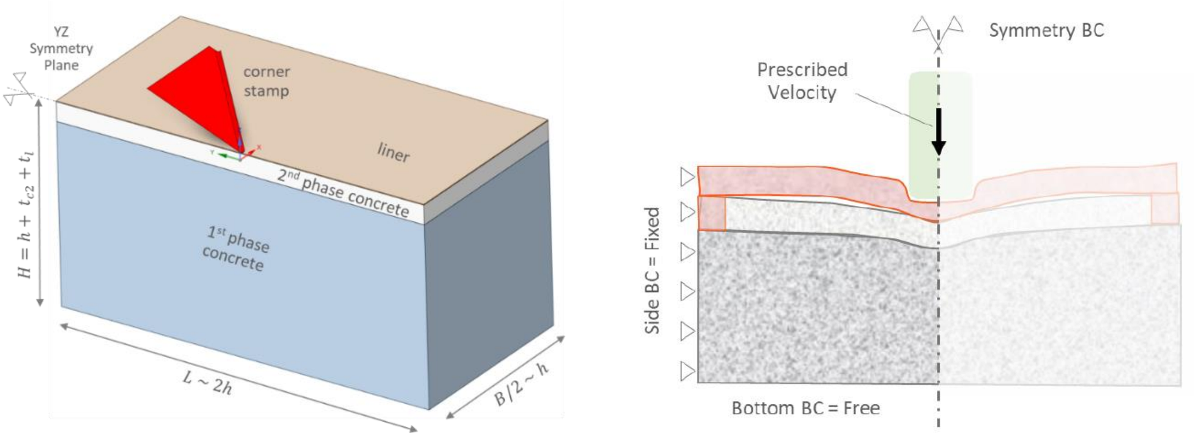

Figure 5. (a) Simulation domain geometry for corner impact, 1/2 symmetry; (b) Boundary conditions: bottom, side and symmetry.

1st and 2nd phase concrete layers are considered as perfectly bonded whereas connection of the stamp to liner and liner to 2nd phase concrete is considered as the frictional surface contact. Frictional coefficients used for the modelling of the frictional contacts are based on the available experimental results. In addition, sensitivity study with varying friction coefficient values was performed and showed that the frictional coefficient values have very limited effect on the global response of the structural system.

Liner, primary and secondary concrete structural parts have been modelled with 3D hexahedral solid elements. Corner stamps are modelled with rigid linear triangular and quadrilateral shell elements. Regular, structured finite element mesh has been used for all case studies. Mesh sensitivity study has been performed and appropriate selective meshing strategy has been utilized to achieve optimal trade-off between the accuracy and efficiency. In general, the mesh is refined in the proximity of the impact zone to capture high deformation, stress and strain gradients.

Material Modelling

Dropping body as an impacting load is modelled as rigid. Liner is made of stainless steel and modelled as the von Mises based elasto-plastic material model with multilinear isotropic hardening.

Material constitute model chosen for numerical modelling of the concrete mechanical behaviour in is the Riedel–Hiermaier–Thoma (RHT) material model, Riedel (2004), as implemented in the ANSYS explicit (AUTODYN) solver, ANSYS (2021). RHT material model is able to represent several important aspects of the mechanical behaviour of the concrete material relevant for the current study: different behaviour under uniaxial compression and tension, increase of the concrete strength under biaxial and triaxial confinement pressure (pressure hardening), proper representation of the triaxial stress state behaviour and third invariant dependence for compressive and tensile meridians, strain hardening and softening, tensile failure, residual strength of the crushed material under confining pressure, strain rate hardening in tension and compression (deactivated in the current study due to quasi-static assumption).

The RHT constitutive model is a combined plasticity and shear damage model in which the deviatoric stress in the material is limited by a generalized failure surface of the form

$$f(p, \sigma_{eq}, \theta, \dot{\varepsilon}) = \sigma_{eq} - Y_{TXC}(p) \cdot R_3(\theta) \cdot F_{cap}(p) \cdot F_{rate}(\dot{\varepsilon}) \,, \tag{4}$$

where p represents hydrostatic pressure, σ_{eq} is equivalent (von Mises) stress, θ is Lode angle, $Y_{TXC}(p)$ is compressive meridian, $R_3(\theta)$ is Lode angle dependence function, $F_{cap}(p)$ cap function closing the elastic surface at high pressures and $F_{rate}(\dot{\varepsilon})$ rate-dependent enhancement factor representing the dynamic increase factor as a function of strain rate $\dot{\varepsilon}$ (deactivated here).

The description of the stress state in the material model relates to three pressure dependent limit surfaces: the elastic limit surface ($Y_{elastic}$), failure surface ($Y_{failure}$) and remaining residual strength surface ($Y_{residual}$) for the crushed material, see Figure 6. Residual strength exists under multi-axial stress states in real structures, where the crushed concrete under confining pressure still retains certain level of shear strength due to friction between the crushed particles. Bi-linear strain hardening is represented in the model through the definition of an elastic limit surface and a "hardening" slope. After failure is initiated, a damage model is used for strain softening, which considers the gradual loss of the load-carrying capacity of material after reaching its ultimate tensile or compressive strength (i.e. failure surface $Y_{failure}$).

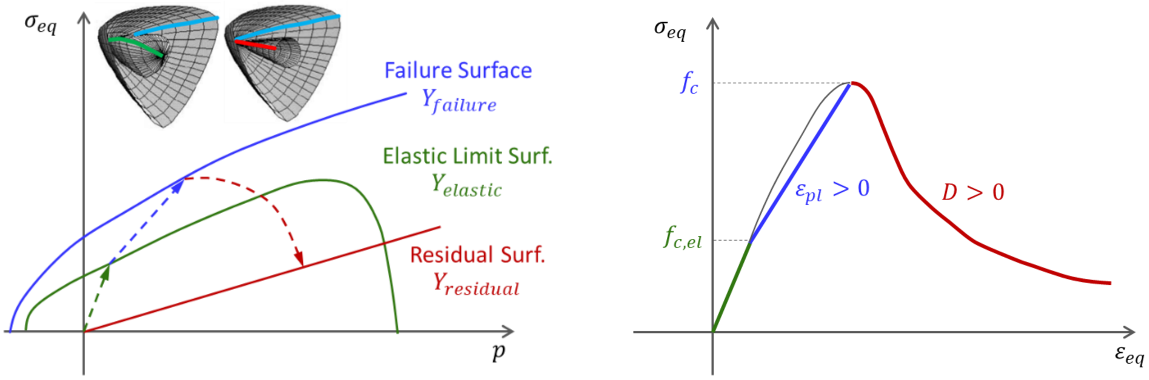

Figure 6. RHT constitutive model: (a) Elastic, failure and residual limit surface; (b) Stress-strain curve in uniaxial compression.

In the current study the standard RHT material model is augmented with two modifications for proper consideration of the behaviour of concrete in low pressure regime, Hu et al. (2016) and Tu et al. (2010). First is the introduction of the Rankine tensile principal stress failure surface which is superimposed onto the original RHT failure surface, and it becomes activated in the lower pressure regime. Second is the introduction of the linear crack softening criteria which considers the specific fracture strain energy as input parameter, enabling the regularization and removal of mesh size dependency effects.

The present study relies on the beyond design assumptions of the material behaviour in order to achieve a realistic behaviour of the concrete subjected to high multi-axial stress states in the proximity of the impact zone. RHT concrete constitutive material model consists of more than 20 material parameters. In the current conceptual design phase, some of the concrete model parameters are calibrated based on the certain code-based material parameters used as a guidance [CEB-FIP (1990,2010), EN 1992-1-1(2004)] while others are estimated from literature data. It should be stressed out that for further detailed studies it is recommended to obtain realistic, test-based material data on the sample specimens of the concrete to be used in the construction of the SFP. This data can be used for more detailed estimation of the concrete constitutive model parameters.

1st phase concrete (CONC1) is defined as high strength concrete, whereas the 2nd phase concrete (CONC2) in its original configuration has a concrete strength equal to 1/3 of the 1st phase concrete. This variant is denoted as CONC2-1/3. As a part of the sensitivity studies, two more 2nd phase concrete variations are considered: concrete with 2nd to 1st strength ratio equal to 2/3 (CONC2-2/3) and 1 (CONC2-3/3).

Quasi-Static Structural Analysis

Explicit time integration using ANSYS explicit, AUTODYN-based, solver has been used for numerical solution of the problem. Time-dependent effects are neglected and the drop load is considered as the equivalent quasi-static load applied as an imposed velocity on the impacting body, essentially corresponding to the applied displacement loading (i.e. displacement controlled experiment). Rate dependent material properties are switched off. Gradual ramp up of the prescribed velocity is made in order to assure that the kinetic energy of the system remains very small compared to the total energy of the system during the entire simulation time, so that the inertia effects would not influence the results. For each of the analysed load cases, stamps are pushed downward until certain target states are reached.

SOLUTION AND ANALYSIS RESULTS

CONC2-1/3 Variant

In the following the normalized characteristic results of the simulation analysis of the drop of the corner of the dropping body are shown. First the results of the 2nd phase concrete variant CONC2-1/3 are given.

Figure 7a shows plots of normalized plastic work of individual structural parts (liner, 1st and 2nd phase concrete) versus normalized vertical stamp force. As the figure indicates, total dissipation energy of the system results mostly from the damage of the 2nd phase concrete. Contribution of the 1st phase concrete to the energy dissipation is negligible.

Figure 7b shows the normalized vertical stamp force versus vertical displacement curve. The maximal achieved force to $R_{cys,b}$ ratio is significantly smaller than 1. This indicates that there is no danger of the punching shear failure and that the shear resistance of the 1st phase concrete has not been exceeded.

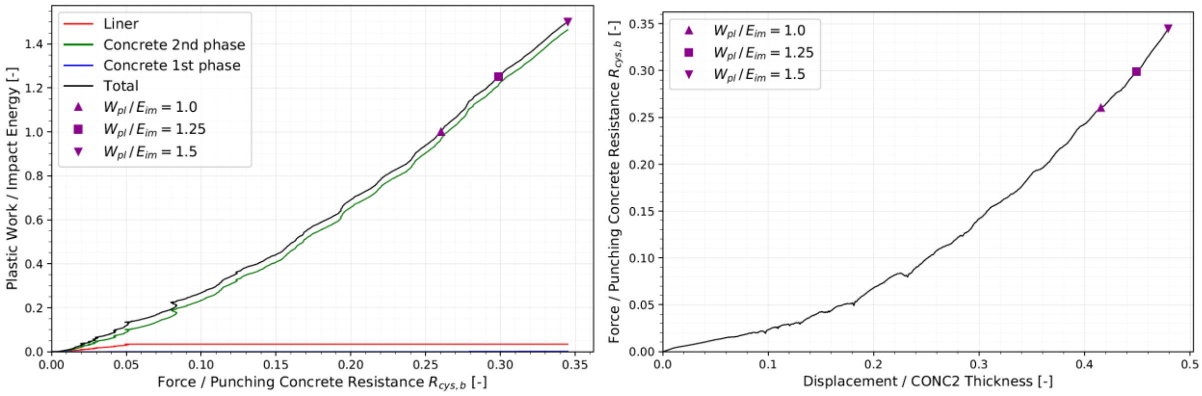

Figure 7. CONC2-1/3: (a) Normalized plastic work vs. force curve; (b) Normalized force vs. displacement curve.

Figure 8 shows a global and local view of the total deformation normalized w.r.t. CONC2 layer thickness at W_{pl}/E_{im} = 1.5 state. As the results suggest, deformations are highly localized in the proximity of the impact. The displacements of the 1st phase concrete are very low, justifying the size of the simulation domain and not modelling of the reinforcement.

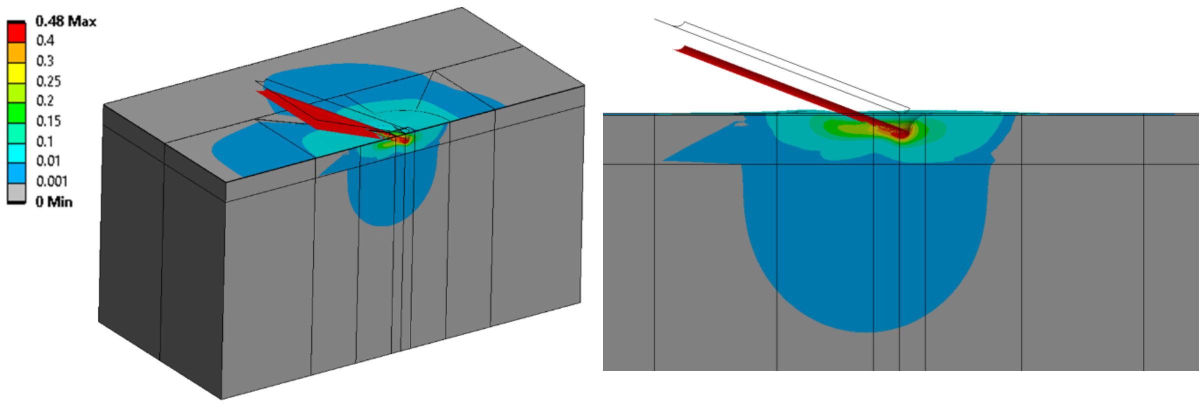

Figure 8. CONC2-1/3 - Normalized deformation contour plots at W_{pl}/E_{im} = 1.5 state: (a) Global view; (b) Local view in the proximity of the impact zone.

Figure 9 shows the distribution of the normalized pressure and equivalent (von Mises) stress in the concrete at W_{pl}/E_{im} = 1.5 state. As can be seen, stress distribution is localized in the proximity of the impact. The stresses quickly dissipate in the area away from the zone of impact. In the zone of impact high confinement pressure state is present resulting in the increase of the maximal peak equivalent stresses to 3.5 times the compression strength of 2nd phase concrete. Post-peak softening behaviour is represented by the evolution of the damage (cracking) or the concrete. After the damage is fully evolved the stress state is governed by the residual strength of completely crushed concrete (representing frictional shear strength under high confinement pressure). On the distal (rear) face low pressure zone is present.

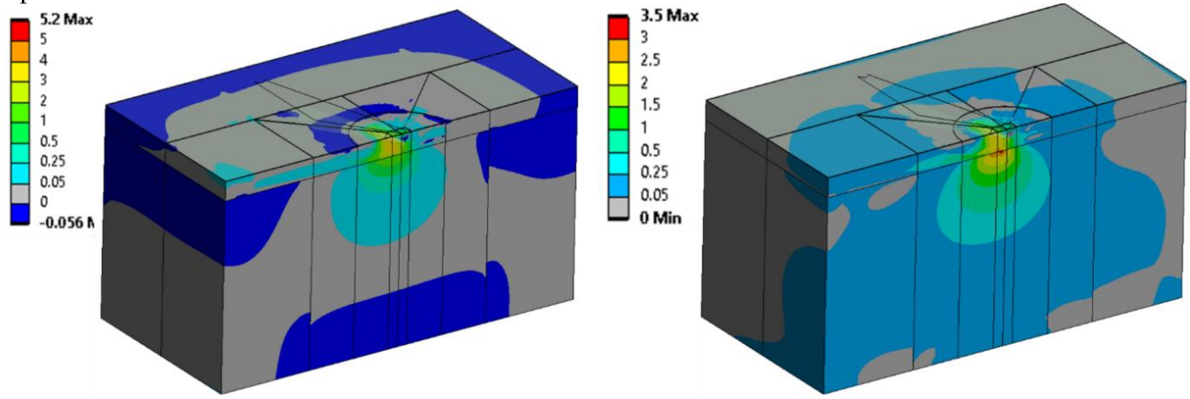

Figure 9. CONC2-1/3 - Normalized stress invariants contour plots at W_{pl}/E_{im} = 1.5 state: (a) Pressure; (b) Equivalent (von Mises) stress.

Figure 10 shows the distribution of the damage in the concrete at three different observation states. High damage occurs in the local area in the proximity of the impact of the 2nd phase concrete. There is no damage occurring in the 1st phase concrete. Low strength ratio of the 2nd to 1st phase concrete acts favourably to the mechanical behaviour of the system. This low strength allows the impact energy to be absorbed and dissipated by the local high inelastic deformations and damage (crushing and cracking) of the concrete. It also protects the 1st phase concrete form cracking, acting as a cushion and "trapping" and containing the damage in this layer. Additionally, 2nd phase concrete enables distribution of the contact pressure at a larger surface area and prevents large concentration of stresses at a small area on the top of the 1st phase concrete.

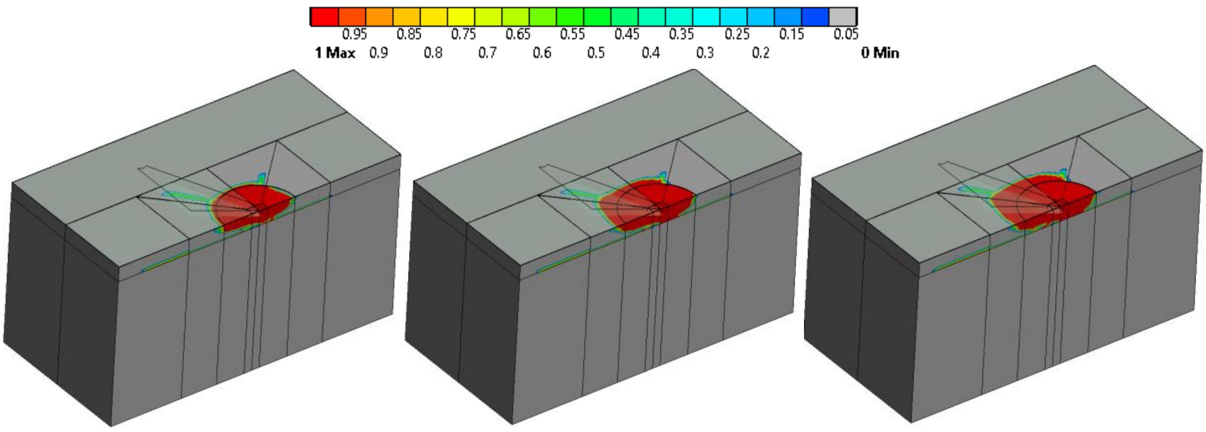

Figure 10. CONC2-1/3 - Concrete damage evolution at different observation states: (a) W_{pl}/E_{im} = 1.0; (b) W_{pl}/E_{im} = 1.25; (c) W_{pl}/E_{im} = 1.5 state.

Sensitivity Study

Results of the sensitivity study on the influence of the strength of the 2nd phase concrete on the mechanical response of the concrete structure are discussed next.

Figure 11a shows sensitivity analysis plots of the normalized plastic work versus normalized vertical stamp force. Figure 11b shows dissipation energy contributions by individual structural parts for CONC2-3/3 case. As for the CONC2-1/3 case (see Figure 7a), the total dissipation energy of the system results mostly from the damage of the 2nd phase concrete. Contribution of the 1st phase concrete is still very low.

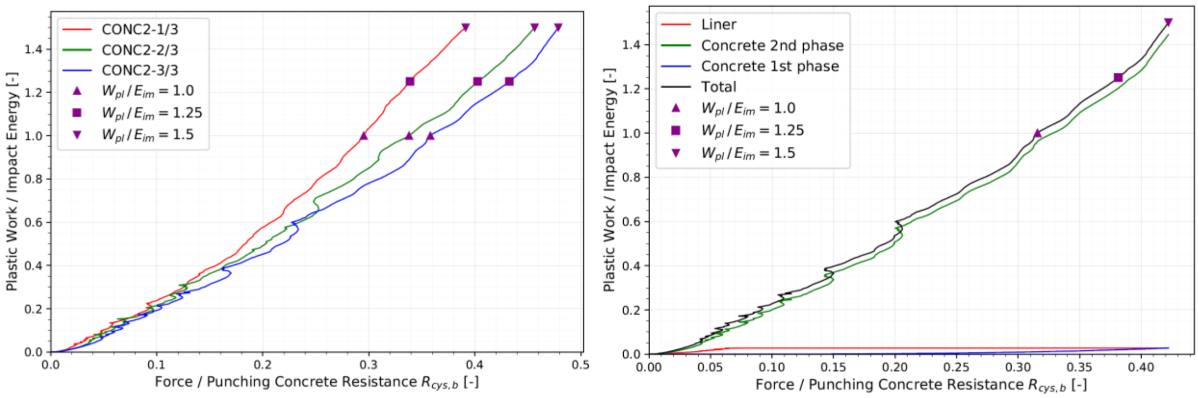

Figure 11. Normalized plastic work vs. force curve: (a) Sensitivity analysis on the effects of the 2nd phase concrete strength; (b) Dissipation energy contributions by individual structural parts for CONC2-3/3 case.

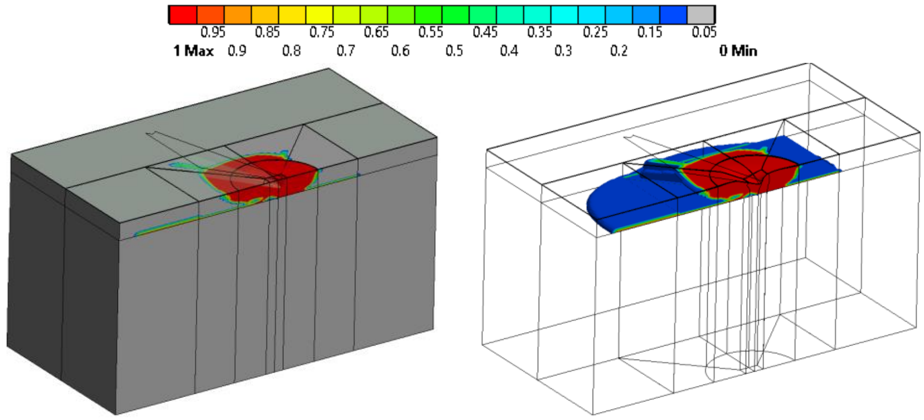

Figure 12. CONC2-1/3 - Concrete damage at W_{pl}/E_{im} = 1.5 state: (a) Exterior; (b) Interior view.

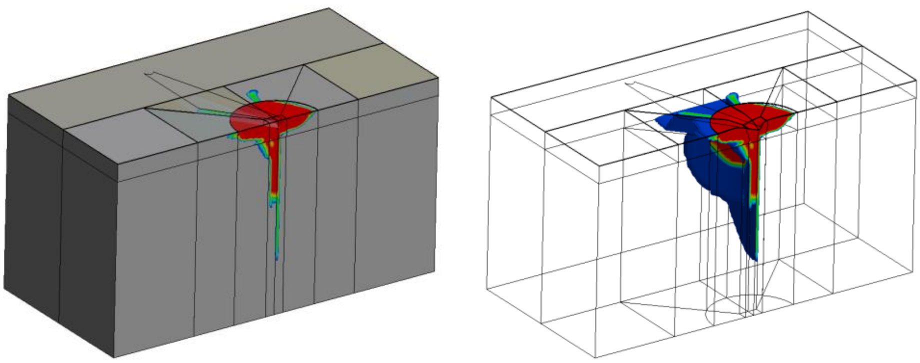

Figure 13. CONC2-2/3 - Concrete damage at W_{pl}/E_{im} = 1.5 state: (a) Exterior; (b) Interior view.

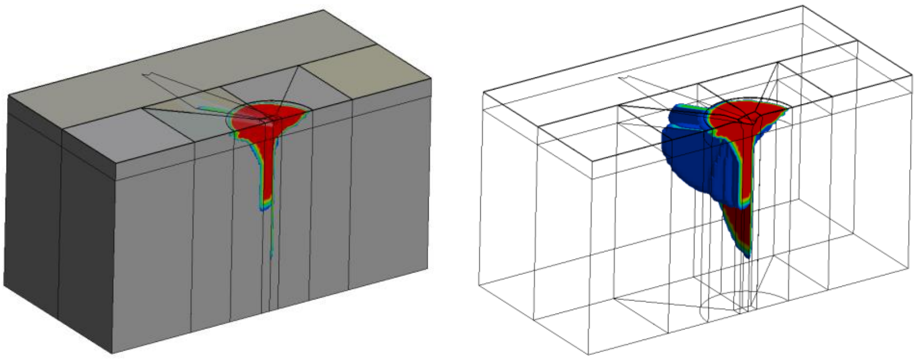

Figure 14. CONC2-3/3 - Concrete damage at W_{pl}/E_{im} = 1.5 state: (a) Exterior; (b) Interior view.

Figures 12 to 14 show the distribution of the damage in the concrete at $W_{pl}/E_{im} = 1.5$ state for three 2nd phase concrete variations. As in the CONC2-1/3 case, high damage occurs in the local area in the proximity of the impact. Damage patterns for CONC2-2/3 and CONC2-3/3 case are similar. It is evident that at higher CONC2 strengths damage is occurring in the 1st phase concrete as well, since the impact is no longer cushioned solely by the 2nd phase concrete. In both cases the 1st phase concrete exhibits moderate local damage with singular cracks propagating almost all the way to the bottom of the pool. Damage is however still limited to singular cracks and there is no danger of the loss of structural integrity.

Failure mode by punching shear through the entire thickness of the 1st phase concrete might not even be possible. Due to a very small impacting area and high slab thickness, damage pattern for CONC2-2/3 and CONC2-3/3 case in the current study resembles that of a projectile impact case with a possible damage evolution scenario which could result in a concrete plugging and eventually shear cone punching limited to the zone in the proximity of the rear face. However, more accurate assessment of the damage pattern would require a more detailed simulation analysis (considering dynamic effects, reinforcement, realistic kinematics of the dropping body and its flexibility and energy dissipation, etc.) and/or experimental tests.

CONCLUSIONS

The results of the analysed drop load cases indicate that, depending on the drop load case, the strength of the 2nd phase concrete layer and associated level of structural damage, analysed spent fuel pool structure is capable of mobilizing enough dissipation energy to withstand the impacting energy. High confinement pressure is present in the proximity of the zone of impact significantly increasing the shear failure strength of the concrete in that area. Sensitivity studies indicate that low ratio of the 2nd to 1st phase concrete strength acts favourably to the mechanical behaviour of the system. Low 2nd phase concrete strength allows the impact energy to be absorbed and dissipated by the local high inelastic deformations and damage (cracking and crushing) of 2nd phase concrete layer. By balancing the ratio of the 1st and 2nd phase concrete strength it is possible to protect the 1st phase concrete from extensive cracking and damage, with 2nd phase concrete layer acting as a controlled crushing layer, containing the damage within.

REFERENCES

ANSYS. (2021). Simulation software ANSYS Version 2021 R2, Ansys Inc., Canonsburg, PA, USA.

CEB. (1988). *Concrete Structures under Impact and Impulsive Loading*, Comité Euro-Inernational Du Béton, Bulletin No. 187, 1988.

CEB-FIP. (1990). *Model Code for Concrete Structures 1990*. Comité Euro-Inernational Du Béton.

CEB-FIP. (2010). *Model Code for Concrete Structures 2010*. Comité Euro-Inernational Du Béton.

EN 1992-1-1. (2004). *Eurocode 2: Design of Concrete Structures – Part 1-1: General rules and rules for buildings*.

Fila, A., Lehmann, F. and Tropp, R. (2015). "Perforation Resistance of Reinforced Concrete Slabs Affected by Low Velocity Drop Loads", *Proc., 23rd Conference on Structural Mechanics in Reactor Technology*, SMIRT-23, Manchester, UK.

Hu, G., Wu, J. and Li, L. (2016) "Advanced Concrete Model in Hydrocode to Simulate Concrete Structures under Blast Loading", *Advances in Civil Engineering*, 2016.

RCC-CW. (2020). *Rules for Design and Construction of PWR Nuclear Civil Works*, AFCEN, 2020 Edition.

Riedel, W. (2004). *Beton unter dynamischen Lasten: Meso- und makromechanische Modelle und ihre Parameter*, Fraunhofer-Institut für Kurzzeitdynamik, Ernst-Mach-Institut, Freiburg, Germany.

Tu, Z. and Lu, Y. (2010). "Modifications of RHT material model for improved numerical simulation of dynamic response of concrete", *International Journal of Impact Engineering*, 37: 1072-1082.